Surface current patterns in the northern Adriatic extracted from high-frequency radar data using self-organizing map analysis

Hrvoje Mihanović,[1] Simone Cosoli,[2] Ivica Vilibić,[3] Damir Ivanković,[3] Vlado Dadić,[3] and Miroslav Gačić[2]

Received 5 March 2011; revised 6 May 2011; accepted 20 May 2011; published 26 August 2011.

[1] A network of high-frequency (HF) radars was installed in the northern Adriatic in the second half of 2007, aimed to measure surface currents in the framework of the North Adriatic Surface Current Mapping (NASCUM) project. This study includes a detailed analysis of current measurements from February to August 2008, a period in which three radars were simultaneously operational. Current patterns and temporal evolutions of different physical processes were extracted by using self-organizing map (SOM) analysis. The analysis focused on subtidal frequency band and extracted 12 different circulation patterns on a 4 × 3 rectangular SOM grid. The SOM was also applied on a joint data set that included contemporaneous surface wind data obtained from the operational hydrostatic mesoscale meteorological model ALADIN/HR. The strongest currents were recorded during energetic bora episodes, being recognized by several current patterns and having the characteristic downwind flow with magnitudes exceeding 35 cm/s at some grid points. Another characteristic wind, the sirocco, was represented by three current patterns, while the remaining current structures were attributed to weak winds and the residual thermohaline circulation. A strong resemblance has been found between SOM patterns extracted from HF radar data only and from combined HF radar and wind data sets, revealing the predominant wind influence to the surface circulation structures and their temporal changes in the northern Adriatic. These results show the SOM analysis being a valuable tool for extracting characteristic surface current patterns and forcing functions.

Citation: Mihanović, H., S. Cosoli, I. Vilibić, D. Ivanković, V. Dadić, and M. Gačić (2011), Surface current patterns in the northern Adriatic extracted from high-frequency radar data using self-organizing map analysis, *J. Geophys. Res.*, *116*, C08033, doi:10.1029/2011JC007104.

1. Introduction

[2] The Adriatic Sea, the northernmost part of the Mediterranean, is a semienclosed marginal basin, approximately 800 km long and 200 km wide and elongated in NW-SE direction (Figure 1). It can be divided into three distinct subbasins, depending on their respective bathymetric characteristics. The southernmost part (South Adriatic Pit) is the deepest (up to 1200 m) and is separated from the middle, 270 m deep Jabuka Pit by the Palagruža Sill (depths up to 170 m). The northernmost part is shallow, with gradual slopes exceeding the depth of 50 m only to the south of the Istrian Peninsula [*Gačić et al.*, 2001].

[3] Surface circulation of the Adriatic Sea has been extensively studied for more than a century and generally a basin wide cyclonic circulation is observed [e.g., *Poulain and Cushman-Roisin*, 2001], with the Eastern Adriatic Current (EAC) flowing along the eastern coast and a return flow occurring along the Italian coast, forming the Western Adriatic Current (WAC). Several recirculation cells are found: two of them topographically controlled in the Middle Adriatic (Jabuka Pit) and in the Southern Adriatic (South Adriatic Pit), and the third, apparently persistent cell, existing in the lower northern subbasin [*Poulain*, 2001; *Ursella et al.*, 2006]. However, numerous studies revealed that the northern Adriatic circulation can be highly variable both in time and space [e.g., *Malanotte-Rizzoli and Bergamasco*, 1983; *Artegiani et al.*, 1997] (see also *Poulain et al.* [2001] for a review) as it is influenced by strong winds in the area, heat and water fluxes on the surface, freshwater input (with the Po River representing the major freshwater source) and a complex relation with the general Adriatic circulation at the southern border.

[4] However, surface current patterns are, for the most part, under a major influence of local wind forcing, especially when wind speed exceeds a certain threshold [*Ursella et al.*, 2006; *Gačić et al.*, 2009]. Major winds affecting the area are the bora (bura in Croatian); northeasterly cold and

[1]Hydrographic Institute of the Republic of Croatia, Split, Croatia.
[2]Istituto Nazionale di Oceanografia e di Geofisica Sperimentale, Sgonico, Italy.
[3]Institute of Oceanography and Fisheries, Split, Croatia.

0148-0227/11/2011JC007104

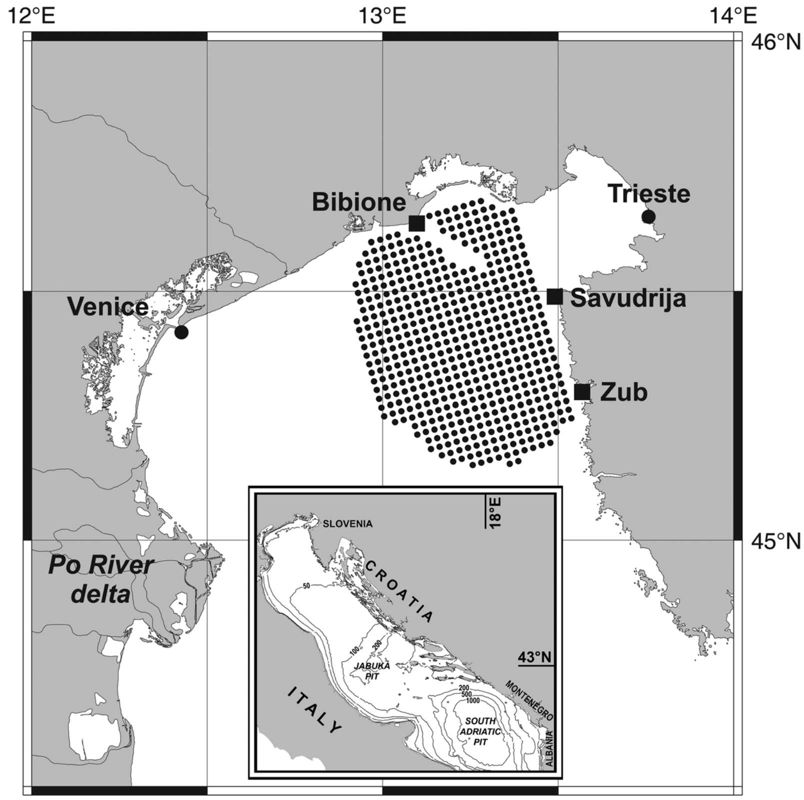

Figure 1. Map of the northern Adriatic showing HF radar points with more than 60% data coverage between February and August 2008. Radar stations (Bibione, Savudrija, and Zub) are denoted by squares. Sea level was measured at Trieste and Venice tide gauges (the latter is located at the Lido inlet, whereas the old city of Venice is lying just underneath the "e" of the Venice label). A map of the whole Adriatic is also inserted.

dry downslope wind, characterized by strong gustiness, being most frequent during winter [*Gačić et al.*, 2001; *Grisogono and Belušić*, 2009], and the sirocco (jugo in Croatian); warm and humid wind blowing from the southeastern quadrant along the major Adriatic basin axis, weaker than bora and particularly influencing the Adriatic in autumn and winter [*Pasarić et al.*, 2007]. Generally, both winds are related to meteorological disturbances moving over the region (see *Poulain and Raicich* [2001] for a review). Observations and numerical studies reveal that bora forcing generates marked contribution to the northern Adriatic circulation, as well as the double-gyre system which forms after a bora event (see *Orlić et al.* [1992] and *Poulain et al.* [2001] for a review). Due to the bora alongshore variability and related wind stress curl, the cyclonic gyre is formed near the head of the Adriatic basin, influencing the advection of the Po River plume to the northeast [e.g., *Orlić et al.*, 1994; *Beg Paklar et al.*, 2001; *Cushman-Roisin and Korotenko*, 2007]. On the other hand, the sirocco enhances the dominant northwestward flow along the eastern coast [*Pasarić et al.*, 2007], but it may temporarily reverse the prevailing southeastward flow along the Italian coast, as confirmed by different measurements and modeling results [e.g., *Orlić et al.*, 1994; *Kovačević et al.*, 2000; *Poulain et al.*, 2004].

[5] A detailed view on mesoscale properties of the Adriatic circulation has been enabled through development of coastal high-frequency (HF) radar measurements. The first deployment of HF radars in the Adriatic took place offshore Ancona at the end of 1990s [*Kovačević et al.*, 2000]. Subsequently, a radar network was set up in front of the Venice Lagoon from November 2001 to November 2005 [*Kovačević et al.*, 2004; *Gačić et al.*, 2009]. At the same time, another HF radar network was operational to the south of the Po River [*Chavanne et al.*, 2007], covering a period between October 2002 and October 2004. The former measurements were compared with ADCP data and, the accuracy of HF radar current data in shallow water was confirmed addressing also observed differences and problems in radar performance [*Cosoli et al.*, 2005, 2010]. *Kovačević et al.* [2004] focused on a detailed description of that network and an explanation of the main circulation properties in front of the lagoon, with specific case studies (snapshots) used to interpret the circulation during different wind conditions. On the other hand, *Gačić et al.* [2009] related the subtidal surface circulation patterns to dominant wind regimes in the area, by applying a conditional averaging approach.

[6] The self-organizing maps (SOM) method is structured as an artificial neural network based on an unsupervised learning [*Kohonen*, 1982, 2001]. It represents an efficient tool for feature extraction and classification and as such it has been applied in diverse research fields, including economy, agriculture, music, robotics etc. [*Richardson et al.*, 2003]. It

has also been widely used in climate and meteorological research [e.g., *Malmgren and Winter*, 1999; *Cavazos*, 2000; *Hewitson and Crane*, 2002; *Reusch et al.*, 2007]. However, it was only recently introduced to oceanography, proving to be particularly useful in extracting interpretable patterns in remotely sensed data sets. *Ainsworth* [1999] and *Ainsworth and Jones* [1999] have applied SOM to improve chlorophyll estimates from satellite data, while *Silulwane et al.* [2001] and *Richardson et al.* [2002] have used SOM to identify ocean chlorophyll profiles. In addition, SOM analyses have also been applied to sea surface temperature (SST), sea surface height (SSH), winds measured by satellite [*Richardson et al.*, 2003; *Risien et al.*, 2004; *Liu et al.*, 2006a, *Liu and Weisberg*, 2007], and ocean currents measured by moored ADCPs and HF radars [*Liu and Weisberg*, 2005, 2007; *Liu et al.*, 2007; *Mau et al.*, 2007]. Two Adriatic SOM-based studies were addressing hydrological and biogeochemical features in the northern Adriatic [*Solidoro et al.*, 2007; *Socal et al.*, 2008], whereas *Vilibić et al.* [2011] made the first attempt to detect patterns in the deep Adriatic water masses and to evaluate the relative usefulness of the SOM compared to other approaches.

[7] Considering the size and complexity of HF radar data sets in general, the SOM proves to be particularly valuable for resolving different physical processes detected in HF radar measurements, while retaining temporal mean fields, allowing for data gaps and successfully extracting asymmetric patterns [*Liu et al.*, 2007]. Therefore, we implemented this approach to map characteristic surface current features in the northern Adriatic, by including not only HF radar data, but also surface wind fields derived from the operational mesoscale meteorological model ALADIN/HR [*Ivatek-Šahdan and Tudor*, 2004]. The data used in the study are introduced in section 2, along with a more detailed description of the SOM. Section 3 focuses on the SOM mapping of HF radar data and joint SOM analysis of HF radar currents and ALADIN/HR wind data. Furthermore, it documents a comparison of the SOM mapping and conditional averaging approach. The SOM solutions, their temporal and spatial characteristics and potential usefulness not only in scientific research, but also in operational oceanography, rapid environmental assessment and forecasts are discussed in section 4.

2. Data and Methods

2.1. HF Radar Data

[8] The analysis presented in this paper is based on surface current measurements obtained by high-frequency (HF) radars installed in the eastern part of the northern Adriatic (Figure 1). The fundamental physical mechanism on which such measurements are based is the Bragg scattering of the electromagnetic radiation over a rough sea [*Crombie*, 1955]. HF radars measure surface currents by detecting the Doppler shift of an electromagnetic wave transmitted at a certain frequency, which scatters on the ocean waves of exactly the half wavelength of the transmitted wave. For HF radars used in this study it means that a 12 m wave (corresponding to a 25 MHz transmitting frequency) is backscattered from the 6 m surface waves [*Paduan and Graber*, 1997]. A single HF radar station determines only the radial component of the surface currents relative to that station. Therefore, two or more radar stations are needed to reconstruct the surface currents field in an area of overlapping coverage. The application of HF radar technology strongly evolved during last 30–40 years, and it now represents a powerful oceanographic tool, especially important in coastal areas [e.g., *Barrick et al.*, 1977; *Paduan and Rosenfeld*, 1996; *Gurgel et al.*, 1999; *Kovačević et al.*, 2004]. One of the major benefits of HF radar measurements is that they allow for multiple ocean parameters (surface currents, surface waves, wind direction etc. [e.g., *Wyatt*, 2005; *Gurgel et al.*, 2006]). Recently, this technology proved to be useful even in assessing high-frequency phenomena, such as tsunamis [*Lipa et al.*, 2006].

[9] Two HF radar stations were installed on the western coast of Istria (Zub and Savudrija) and were operational since August 2007, providing the data in real time, while the third station (Bibione–Punta Tagliamento) located on the Italian coast was added to the network in December 2007. The entire network was created in the framework of the NASCUM (North Adriatic Surface Current Mapping) project [e.g., *Vilibić et al.*, 2009]. The network sites were equipped with the SeaSonde HF radar systems produced by Codar Ocean Sensors (COS), working in the 25 MHz frequency band with a 100 kHz bandwidth (1.5 km resolution in range). Operating settings enabled a maximum operating range of each antenna up to 50 km, with a 5° angular resolution. The nominal accuracy of total vectors as specified by the producer is less than 7 cm/s in magnitude and less than 10 degrees in direction [*Kovačević et al.*, 2004].

[10] Hourly surface current vectors were derived over a regular grid having a horizontal resolution of 2 km × 2 km. A least squares approach was used, and radial velocities from at least two sites were mapped onto a described grid [*Lipa and Barrick*, 1983; *Barrick and Lipa*, 1986]. Whenever available, the data from the third radar were included to give better spatial coverage and more reliable measurements. It is important to emphasize that the mapping procedure excluded surface current vectors with large geometrical dilution of precision caused by poor intersecting beam geometry [*Chapman and Graber*, 1997]. Moreover, grid points with an insufficient number of radial velocities from each site were also removed, and total current vectors having magnitude larger than 1 m/s were excluded from the record. The resulting data of vector current components were checked for spikes and then processed as described by *Kovačević et al.* [2004]. Some of the points close to the baseline between Bibione and Savudrija were missing because of poor intersecting beam geometry: Figure 1.

[11] Preliminary analysis of the entire data set (August 2007 to August 2008) was performed both in time and frequency domain, at points having at least 50% data coverage. At each grid point data gaps were filled in using linear interpolation or weighted averages of observations from surrounding locations when necessary. The T-Tide Matlab package was used to perform the tidal analyses on the noninterpolated current vectors [*Pawlowicz et al.*, 2002]. Since tides turned out to be relatively weak, contributing less than 20% to total current variance (S. Cosoli et al., Surface current variability and wind influence in the northeastern Adriatic Sea from high-frequency (HF) radar measurements, submitted to *Continental Shelf Research*, 2011), subtidal currents analyzed in this paper were resolved by applying a 4th order Butterworth low-pass filter on

interpolated currents, with a cutoff period of 33 h [e.g., *Emery and Thomson*, 1997]. When there were larger gaps in original time series, shorter data sets were filtered separately, and the series were reconstructed with gaps preserved.

[12] This paper attempts to give a detailed investigation of surface current patterns in subtidal frequency band, by applying the self-organizing maps (SOM) method on hourly current fields and joint data array which includes surface wind data obtained from the operational model ALADIN/HR. We focused on the period when three network radars were operational for the longest intervals (February–August 2008). Given that temporal and spatial gaps may render the results unreliable if they persist over a long period or over too large an area [*Liu et al.*, 2007] we choose to include only those grid points that have a 60% or higher data coverage (marked by small dots in Figure 1).

2.2. ALADIN/HR Fields

[13] The Aire Limitée Adaptation dynamique Développement International (ALADIN) model is a hydrostatic, primitive equation model developed within an international cooperation involving fifteen National Meteorological Services. The model was developed from a global ARPEGE (Action de Recherche Petite Échelle Grande Échelle) model [*Courtier et al.*, 1991]. The analysis and forecast of the ARPEGE provides initial and boundary conditions for ALADIN. The ALADIN model is being run operationally on a daily basis on different domains by the participating countries. The ALADIN/HR is run at 00 and 12 UTC by the Croatian Meteorological and Hydrological Service, on a domain encompassing the Adriatic Sea and adjoining countries [*Ivatek-Šahdan and Tudor*, 2004]. The ALADIN/HR horizontal resolution is 8 km, with 37 sigma levels unequally spaced in the vertical.

[14] A high-resolution dynamic adaptation of the model, which adapts operational ALADIN/HR wind fields to a 2 km resolution, is also available [*Ivatek-Šahdan and Tudor*, 2004]. Due to a finer resolution, it includes more detailed terrain topography and the land-sea mask and surface properties. High-resolution ALADIN/HR surface wind fields (at 10 m) over the Adriatic were available at 3 h interval for the entire HF radar operational period (August 2007 to August 2008). These time series were interpolated to hourly values and filtered by the aforementioned low-pass filter. As a result, a combined data set consisting of surface current fields and ALADIN/HR wind data was created, thus resolving an input data array for the SOM.

2.3. Wind and Sea Level Time Series

[15] The time series from a selected ALADIN/HR grid point to the south of the line connecting Bibione and Savudrija (λ = 13.27°E; φ = 45.5°N) were also examined to interpret the results of the SOM analyses. Moreover, our investigation included sea level data measured at Trieste and Venice tide gauges, in order to relate sea-surface variability in the northern Adriatic with diverse wind forcing and corresponding surface current patterns. The data from Italian tide-gauge stations are freely available from ISPRA (The Institute for Environmental Protection and Research, Italy, http://www.mareografico.it). Sea level measurements were carefully checked, interpolated where necessary and time series were low-pass-filtered (33 h LP) to remove tides and Adriatic Sea seiche signals, which have periods of about 21 and 11 h [*Buljan and Zore-Armanda*, 1976; *Vilibić*, 2006]. High frequency variability in ALADIN/HR wind time series (mainly diurnal oscillations due to a sea-breeze regime (Cosoli et al., submitted manuscript, 2011)) was removed by the same low-pass filter that was applied to the current and sea level data. These series were related to surface current fields by analyzing different wind-forcing conditions (bora, sirocco, other winds and calm) and applying conditional averaging approach as described by *Gačić et al.* [2009].

2.4. Self-Organizing Maps

[16] As an artificial neural network, the SOM learns by an iterative process through which input data are presented successively to the network [*Kohonen*, 1982, 2001]. Initially, the units (nodes) can be randomly distributed in the data space. The input data are then sequentially presented to the network and the activation of each unit for the presented input vector is calculated using an activation function (usually the Euclidean distance between the weight vector of the unit, and the input vector). In each successive step the weight vector of the unit showing the highest activation (i.e., the smallest Euclidian distance) is selected as the "winner," or the best matching unit (BMU), and is modified to more closely resemble the presented input vector [e.g., *Liu and Weisberg*, 2005]. Moreover, the weight vectors of neighboring units are also modified according to a spatial-temporal neighborhood function [*Kohonen*, 1982, 2001]. This procedure enables that similar patterns are mapped onto neighboring regions on the map. Generally, input vectors are multidimensional and to visualize their corresponding patterns they are usually mapped onto a low-dimensional (usually 2D) array [*Richardson et al.*, 2003].

[17] Detailed explanations on the SOM method are given by *Richardson et al.* [2003] and *Liu and Weisberg* [2005]. A user friendly version of the SOM toolbox has been provided by *Vesanto et al.* [2000] and the MATLAB toolbox version 2.0 can be downloaded from the Helsinki University of Technology, Finland: http://www.cis.hut.fi/projects/somtoolbox. The toolbox also provides two quantitative measures of mapping quality: average quantization error (QE) and topographic error (TE). The QE is the average distance between each data vector and the BMU and it demonstrates the quality of mapping. The TE represents the percentage of the data vectors for which the first BMU and the second BMU are not neighboring units. Lower QE and TE values indicate better mapping quality, although TE is not a critical measure of topographical deficiency for small size SOM like the one used in this study. Still, it can become relevant for large size SOM, as the data set complexity increases [*Liu et al.*, 2006b].

[18] Several authors have outlined the advantages of the SOM over other conventional methods (such as empirical orthogonal function, EOF or principal component analysis, PCA) in extracting characteristic patterns from complex meteorological and oceanographic data sets [*Liu and Weisberg*, 2011]. *Liu and Weisberg* [2005, 2007] showed that the SOM patterns were more accurate than the leading mode EOF patterns in an analysis of ocean current patterns extracted from long time series of currents from a moored

ADCP array. This proved especially important for identifying asymmetric features between upwelling and downwelling patterns, which were successfully extracted by the SOM, but not easily recognized by the (linear) EOF. Moreover, *Liu et al.* [2006b] demonstrated that the SOM was efficient in extracting all complex patterns from multiple artificial data sets, while the EOF failed to do that. Finally, *Mau et al.* [2007] examined 1 year long HF radar observations of Long Island Sound outflows and identified characteristic synoptic flow patterns using the manual classification, the SOM analysis and the EOF decomposition. The SOM patterns were remarkably similar to manually resolved features, demonstrating significant improvement in respect to the EOF classification. In addition, they accentuated the importance of examining the relationship between the SOM patterns and winds.

[19] It should be emphasized that the EOF preserves variance, thus forming a complete set from which the data may be identically reconstructed, whereas the SOM preserves the data topology. While the resulting patterns may be more similar to the data than the leading EOFs, there is no convenient way to exactly reconstruct the data [*Liu et al.*, 2006b].

[20] *Liu et al.* [2006b] also carried out a performance evaluation of the self-organizing map for feature extraction. Their choice of SOM parameters was tested and applied in this study, specifically focusing on the following issues:

[21] 1. Map size: smaller size gives more general information, larger size enables more detailed information.

[22] 2. Lattice structure: rectangular lattice is preferable for small size SOMs and a hexagonal is useful for larger map sizes. "Sheet" map shape is usually used.

[23] 3. Initialization: the initialization of node weights can be random or linear. Linear represents an EOF decomposition and linear interpolation of the first two leading EOFs. This choice saves iteration time (especially with more complex data sets) and provides for better SOM results (fewer iterations for QE convergence and smaller TE [*Liu et al.*, 2006b]). Random initialization was tested as well and resulted in longer QE stabilization and slightly larger TE.

[24] 4. Neighborhood function: previous experiments confirmed that among four neighborhood functions available in the toolbox, the Epanechnikov "ep" neighborhood function with batch training algorithm gives the best results (smallest QE and TE [*Liu et al.*, 2006b, 2007]). Batch algorithm proved to be computationally more efficient than the sequential version [*Vesanto et al.*, 2000].

[25] Therefore, the following parameter choices were applied in this paper: 4 × 3 array (12 patterns) providing a good compromise between details and visualization, a rectangular neural lattice of "sheet" shape, linear initialization, the "ep" neighborhood function and batch training algorithm. The number of iterations was set to 10 (resulting in QE convergence), while initial and final radii of the "ep" function were set to 2 and 1, respectively.

3. Results

3.1. Surface Current Patterns Resolved From HF Radar Measurements

[26] There were 524 HF radar grid points with data coverage over 60% in February–August 2008 period (Figure 1) and the input matrix consisted of 1048 columns (524 points × 2 components) × 5112 rows (hourly time series). Each velocity component was normalized by its standard deviation prior to analysis, so that the different variable ranges do not affect the SOM solution. Vector components were scaled back by their standard deviations after the SOM procedure. The 12 patterns were extracted (as a 4 × 3 array) and they are shown in Figure 2. The most differing patterns are positioned at opposite sides of the array. The efficiency of the SOM in resolving asymmetric current patterns is also evident, with the most energetic patterns (BMU1 and BMU4) positioned in the same array column of the SOM, since the dominant winds (bora and sirocco) are perpendicular in the area. The mapping resulted in quantization error (QE) convergence, with an overall QE of about 121 and a topographic error (TE) close to 23%.

[27] The grouping of similar SOM units is particularly important to better understand the analyzed data sets [*Vesanto and Alhoniemi*, 2000]. Subtidal current structures within the observational domain were horizontally inhomogeneous and the clustering method included in the SOM toolbox (*k*-means clustering) divided the patterns in three distinctive groups. The first group represents strong westward and southwestward surface flow from the Gulf of Trieste along the northern Italian coast (with surface currents surpassing 35 cm/s at some grid points) accompanied by decreasing westward flow further to the south (SOM units 1, 2, and 5: 20.5% of the total occurrence). As observed from ALADIN/HR wind data and BMU time series (the sequence of the BMUs on the *y* axis was rearranged according to the results of the clustering, thus enabling better visual correlation between the winds and the BMU evolutions: Figure 3), these patterns are related to the development of strong bora winds in the area (e.g., 7–13 February 2008, 4–8 March 2008). The winds in this paper are presented in oceanographic convention; that is, the vectors are pointing in the direction of the wind blowing. The second group is characterized by a uniform and less intense northward and northeastward surface current flow along the western Istrian coast, weakening and rotating to the west close to the northern Italian coast (SOM patterns 3, 4, and 8: 23.1% overall occurrence). These SOM units can be ascribed to the sirocco driven surface currents (e.g., 14–18 May 2008) reaching 15 cm/s in BMU4 (Figures 2 and 3). Finally, the remaining six patterns covered 56.4% of the analyzed period (BMUs 6, 7, 9, 10, 11 and 12), and they were characterized by relatively weaker subtidal surface currents. They could be connected with the transient flow, calm intervals and residual thermohaline circulation (as they occur mostly in periods between stronger wind episodes or during intervals with weak winds and calm).

[28] Thus, the SOM analysis confirmed that the pronounced wind forcing seems to be dominant in subtidal surface dynamics in the northern Adriatic [*Ursella et al.*, 2006; *Gačić et al.*, 2009]. Having in mind that the usefulness of the SOM is of particular importance in the analysis of joint complex data sets [e.g., *Liu et al.*, 2007] we applied it on the vector time series containing surface current HF radar measurements and ALADIN/HR surface wind fields in the northern Adriatic.

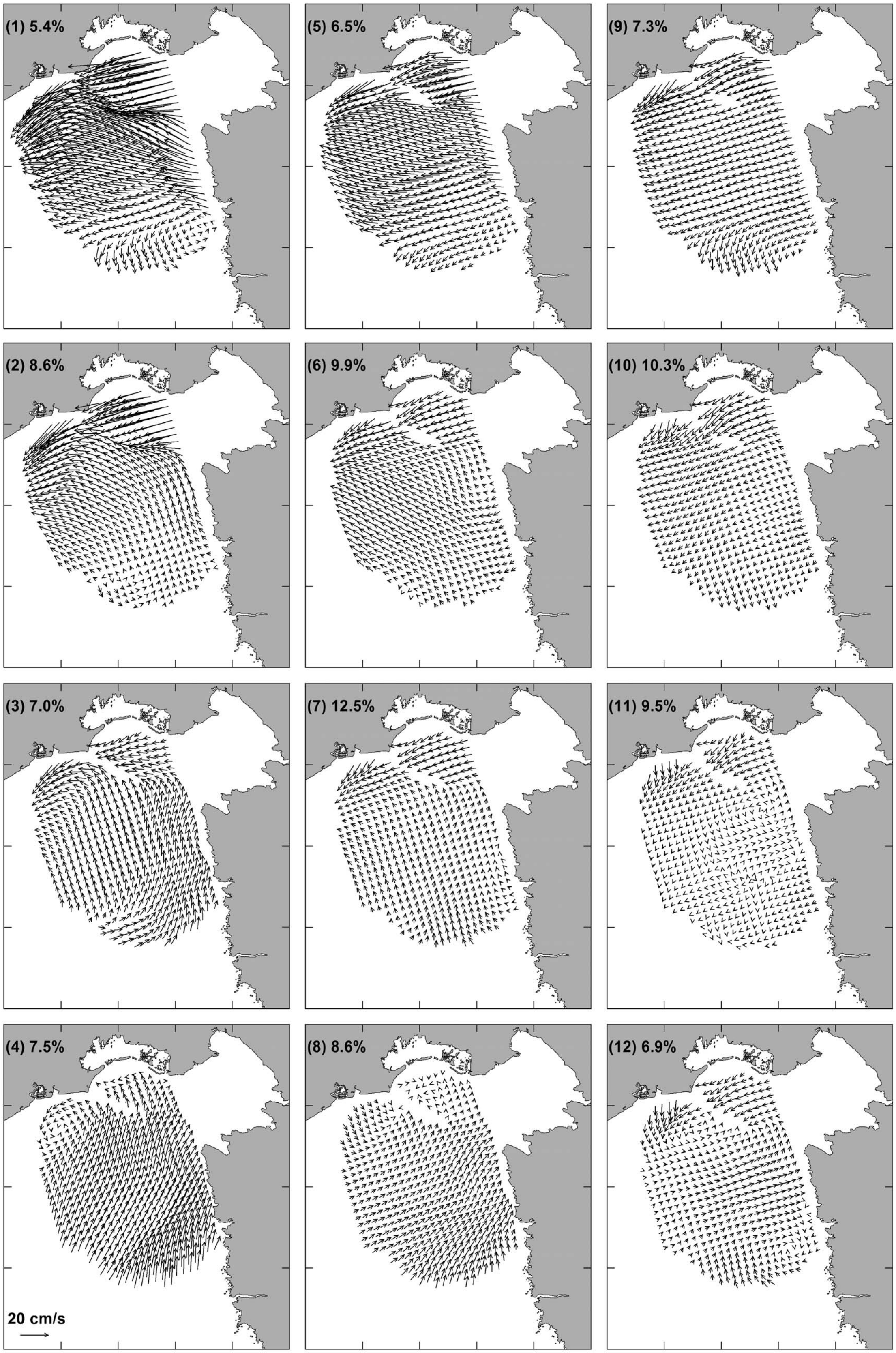

Figure 2. Characteristic spatial patterns of subtidal surface currents extracted by a 4 × 3 SOM analysis of HF radar data from the February–August 2008 period. The relative frequency of occurrence of each pattern is shown in the upper left corner of each respective unit.

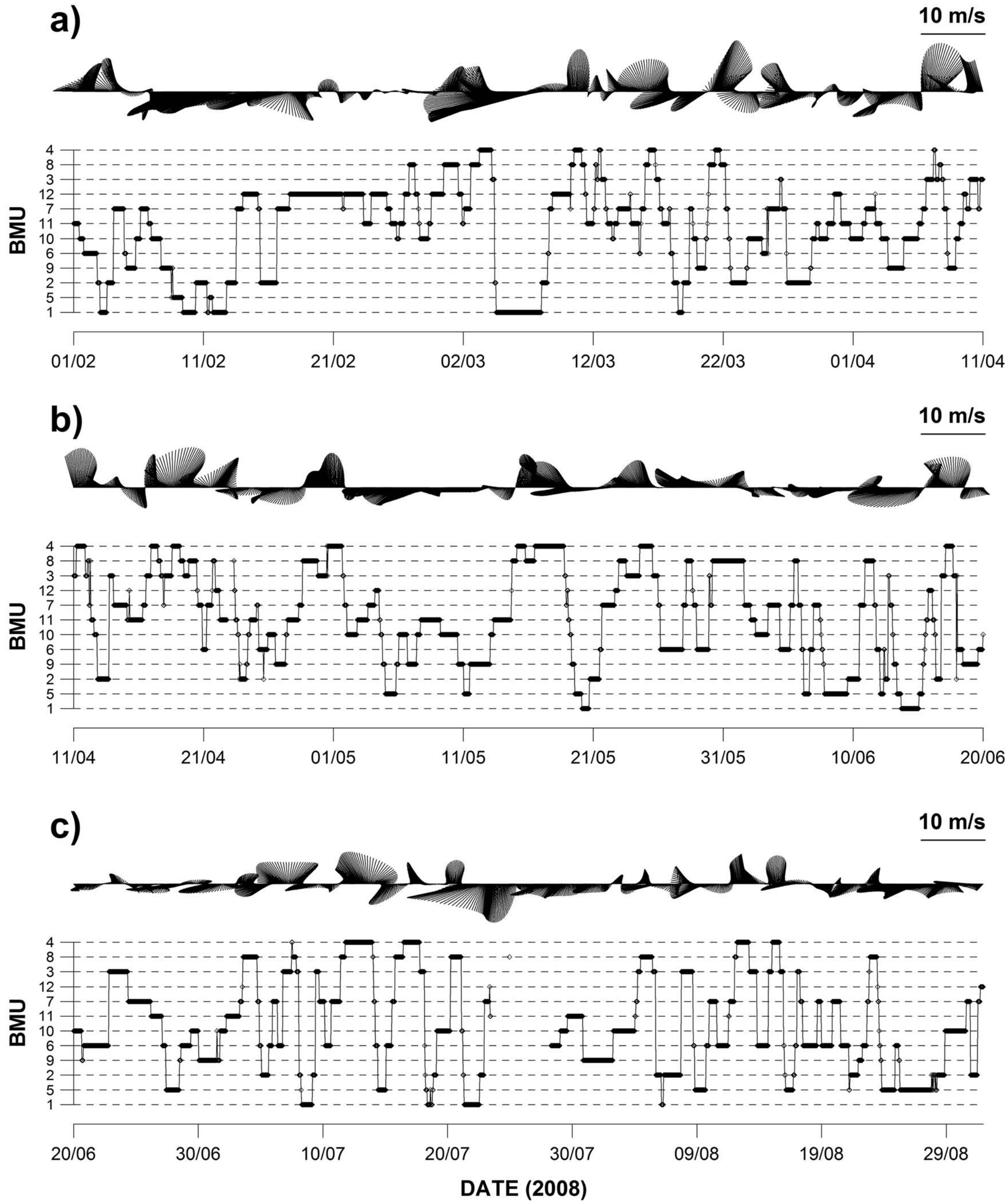

Figure 3. (a) (top) The 33 h low-pass-filtered winds (oceanographic convention) from the select ALADIN/HR grid point and (bottom) temporal evolution of best matching units extracted by a 4 × 3 SOM and presented in Figure 2 for the period between 1 February and 10 April 2008. (b) Same as in Figure 3a, for the interval extending from 11 April to 19 June 2008. (c) Same as in Figure 3a, for the interval between 20 June and 31 August 2008. The sequence of the BMUs on the *y* axis was rearranged following the results of the clustering. This enables better visual correlation between the winds and the BMU evolutions.

3.2. Surface Current Patterns From Joint SOM Analysis of HF Radar Data and ALADIN/HR Surface Winds

[29] Low-passed ALADIN/HR winds were subsampled to 8 km grid, since the high-resolution fields did not include any significant differences in general wind characteristics over the area. Therefore, 364 columns were added to the previously described input matrix (13 longitude points × 14 latitude points × 2 components). Characteristic surface current fields and their temporal evolution turned out to be very similar to the ones resolved by the SOM excluding ALADIN/HR fields (Figures 2 and 4), once again stressing the importance of winds in subtidal surface dynamics. The

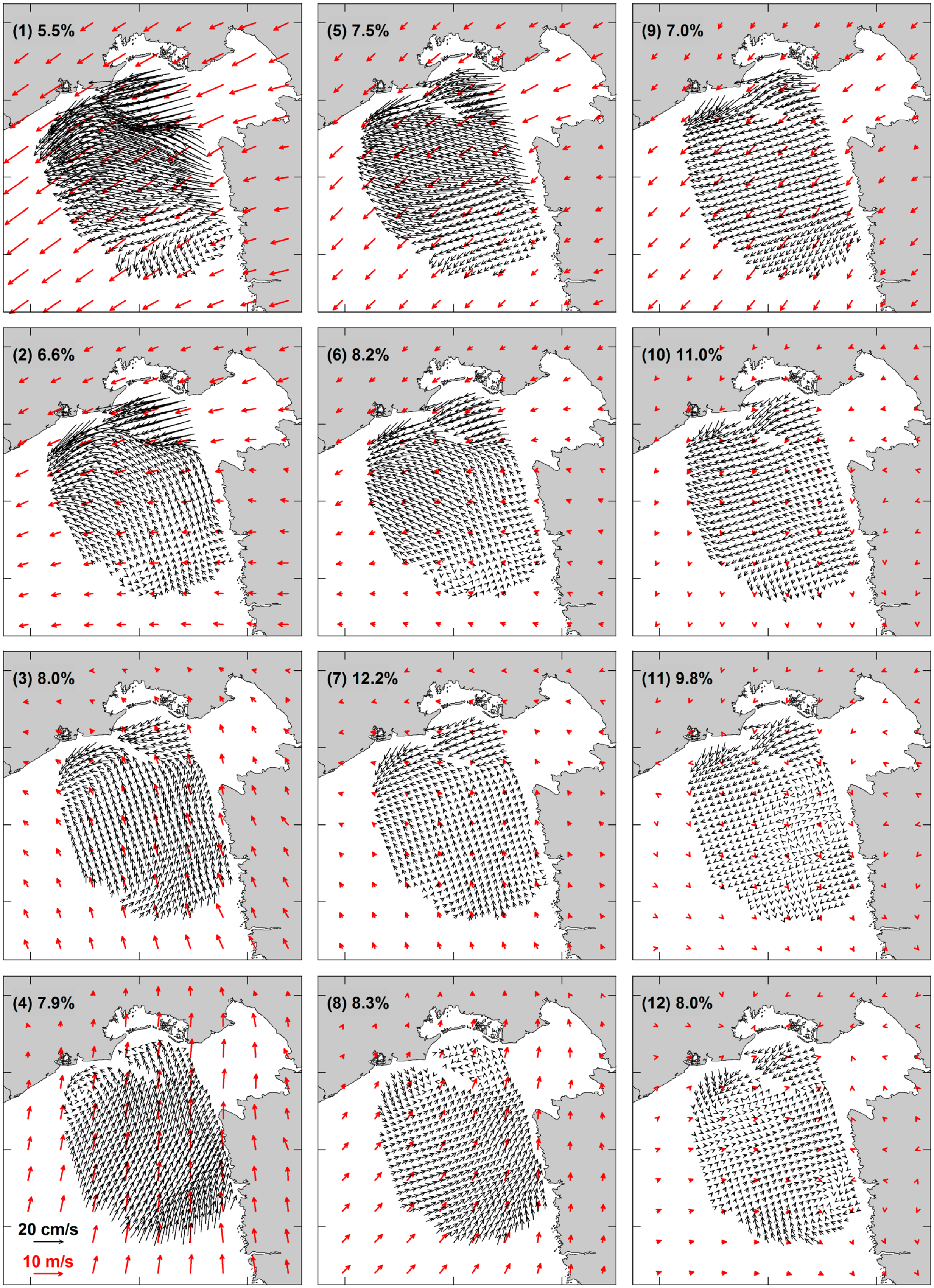

Figure 4. Same as in Figure 2 but for a joint SOM analysis of HF radar measurements and ALADIN/HR wind data. Surface current patterns are denoted by black vectors, whereas the corresponding ALADIN/HR fields are indicated by red vectors.

Table 1. Complex Correlation Coefficients and Respective Veering Angles Between SOM Vector Patterns Derived From Subtidal HF Radar Measurements and Corresponding Features Extracted From Joint SOM Analysis of HF Radar and ALADIN/HR Data[a]

Best Matching Unit	Complex Correlation Coefficient	Veering Angle (Degrees)
1	0.999	−1.15
2	0.991	−0.04
3	0.981	−6.06
4	0.998	1.95
5	0.993	0.99
6	0.932	5.47
7	0.977	1.89
8	0.983	1.57
9	0.896	1.60
10	0.880	−0.99
11	0.949	4.63
12	0.965	−3.86

[a]The patterns related to the bora are 1, 2, and 5, the sirocco structures are 3, 4 and 8, while the remaining SOM units correspond to weak winds and calm and residual thermohaline circulation.

similarity was confirmed by estimating the correlation between HF radar patterns and HF radar + ALADIN/HR patterns, using a complex correlation coefficient [*Kundu*, 1976] together with the mean angular offset of veering (Table 1). The highest correlation was found between characteristic wind patterns, especially between the most pronounced ones, i.e., BMU1 (bora) and BMU4 (sirocco). Absolute values of veering angles were smaller than 6° for all evaluated SOM structures. Moreover, the QE and TE for the joint mapping were lower than the respective mapping quality measures in the SOM analysis of HF radar data only, with QE being around 113, and TE close to 13% in joint analysis.

[30] Previously investigated patterns describing the bora, sirocco and calm periods were also recognized in joint SOM analysis, with slightly different overall occurrences (19.6, 24.2 and 56.2%, respectively). Besides characteristic subtidal surface current fields, Figure 4 includes the corresponding low-frequency wind patterns.

[31] The meridional wind shear observed during the strongest bora pattern (BMU1), with maximum winds at the latitude of the Gulf of Trieste and weaker winds further to the south, resulted in a strong westward jet along the northern Italian coast. The jet was accompanied with a pronounced current shear in the southern part of the domain, thus introducing a significant cyclonic vorticity in the central area. Surface currents were consistent with Ekman dynamics in the central area, but on the southeastern corner of the investigated area (to the southwest of Cape Zub) an indication of weak cyclonic recirculation can be observed, in the most pronounced bora pattern (BMU1).

[32] On the other hand, the strongest sirocco wind pattern (BMU4) was much more uniform, with less intense winds over the area. The resulting currents were consequently more homogenous, dominated by uniform northward flow along the western Istrian coast, veering clockwise with respect to the prevailing wind, and entering the Gulf of Trieste close to Cape Savudrija. Still, the currents become weaker and change direction to the west in the northernmost part, with a small-scale cyclonic eddy being formed on the northwestern corner, close to Bibione. A general clockwise veering of the currents in respect to the wind qualitatively agrees with Ekman theory.

[33] Calmer intervals, which covered about 56% of the measurements in the February–August 2008 period, were characterized by low-intensity nonuniform winds and relatively weak subtidal surface currents.

[34] To give a more detailed insight in the temporal evolution of different patterns, three characteristic intervals were chosen and presented in Figures 5–7. Figures 5–7 include low-pass wind data from a selected ALADIN/HR point in the study area, low-pass-filtered sea levels from Trieste and Venice and simultaneous BMU time series determined from the joint SOM analysis. The first interval encompasses several bora episodes in the first part of February 2008 and a prolonged period of calm weather at the end of the month (Figure 5). Initially, bora was blowing around 3 February (BMU sequence 2→1→2), followed by a short and moderate sirocco on 4 February and a sea level rise at both tide gauge stations. Two other bora episodes occurred between 8 and 13 February (sequence 5→1→2→1→2) and from 15 to 17 February (SOM unit 2), followed by a prolonged calm period (mostly described by patterns 12, 7 and 11). In addition to the cessation of the bora, high-pressure field strengthened over the Adriatic, causing extremely high atmospheric pressure values as observed on 17 February 2008 (above 1045 hPa [*Meteorological and Hydrological Service of Croatia*, 2008]). Conversely, sea level dropped at its absolute minimum values at some station along the eastern Adriatic coast on 17–18 February 2008 (e.g., Rovinj in the northern Adriatic [*Hydrographic Institute of the Republic of Croatia*, 2010]). Low-pass-filtered values at Venice and Trieste were more than 40 cm below the respective annual mean (Figure 5).

[35] The strongest bora episode occurred between 4 and 8 March 2008 with ENE hourly winds reaching 14.5 m/s in the study area (Figure 6). It was preceded by a 2 day sirocco. The largest part of the bora interval was described by BMU1 pattern, with short (transient) BMU2 periods at the beginning and the end of the episode. The SOM results illustrate that surface response to the strong bora wind in the area was almost instantaneous, as already found by *Book et al.* [2005] and *Ursella et al.* [2006]. Sea level change was also evident, with the sea retreating from the Gulf of Trieste and piling up along the northwestern Italian coast. The sea level at Venice was almost 20 cm higher than at Trieste on 5 March 2008 (Figure 6). This bora period was followed by several intermittent sirocco episodes. The strongest two were centered on 10 and 16 March 2010 (BMU4).

[36] The most pronounced sirocco event took place from 15 to 18 May 2008, when southeasterly and southerly winds reached 6.2 m/s at the select ALADIN/HR grid point (Figure 7). The current patterns evolved in the SOM unit sequence 8→4→8→4→3→4→3, consistent with the evolution of the sirocco during the event. A continuous sea level rise was observed at both stations, with the maximum values occurring on 18 May 2008. After a short transient period, the sirocco was succeeded by the bora (blowing from ENE) lasting from 19 to 21 May 2008, with a typical SOM unit sequence illustrating the strengthening, maximum and weakening of northeasterly and easterly winds (5→1→2).

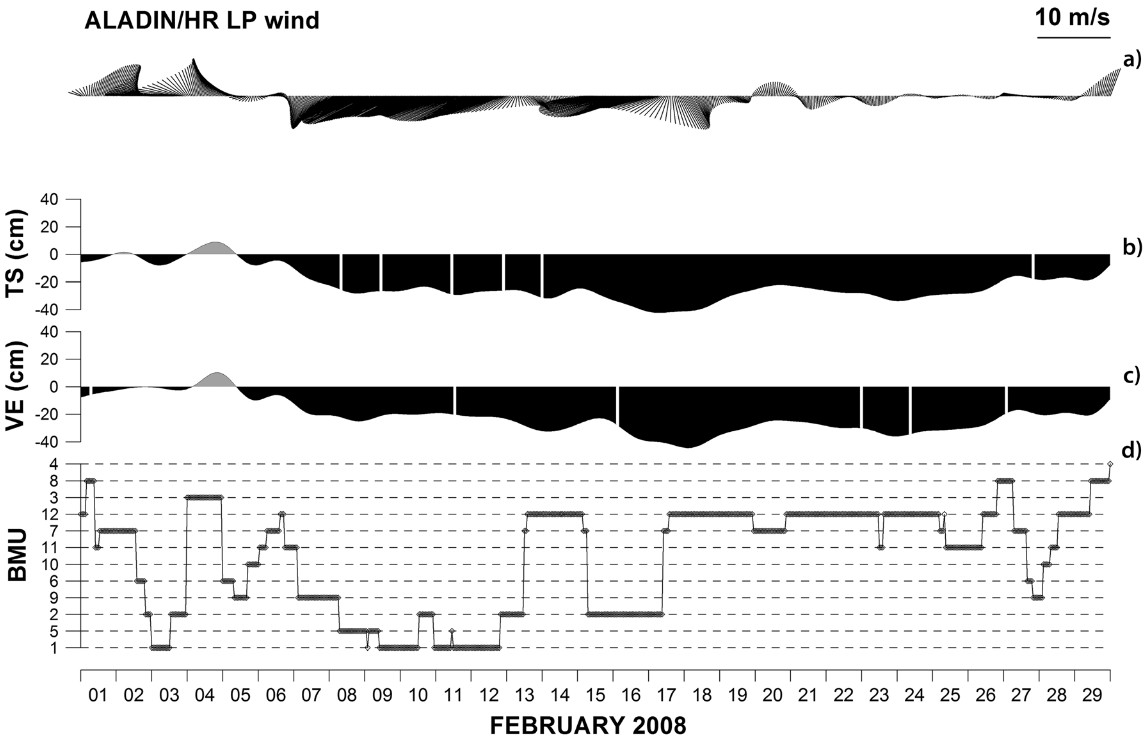

Figure 5. (a) The hourly wind speeds from the select ALADIN/HR grid point and the 33 h low-pass-filtered sea levels at (b) Trieste (TS) and (c) Venice (VE) during February 2008. (d) Temporal evolution of best matching units extracted by a 4 × 3 joint SOM presented in Figure 4.

[37] Generally, less pronounced bora related SOM units (BMUs 2, 5) could be ascribed to the weaker bora episodes or they occur during transitional periods before and after the most severe bora events (BMU2 often takes place during short intervals prior and subsequent to BMU1, with the longer duration in the later phase: Figures 5 and 6). Conversely, transient sirocco associated BMUs (3 and 8) seem to reflect changing conditions between the sirocco and the bora regimes (BMU3) and an intensification of the SE winds (BMU8).

3.3. Comparison With Conditionally Averaged Currents

[38] Another approach in detecting surface current patterns was applied by *Gačić et al.* [2009] on HF radar data measured from February 2004 to February 2005 in front of the Venice lagoon. They divided the study period into three different wind regimes, depending on the speed and direction of prevalent winds. The threshold for other winds and calm was 3 m/s, while bora and sirocco were defined as stronger winds blowing from NE and SE quadrant, respectively. After resolving the intervals related to a certain wind regime, they calculated conditionally averaged currents (CAC) for different wind-forcing conditions.

[39] We used a similar approach in this study to compare conditional averaging with the results obtained by joint objective mapping. Based on the low-passed wind rose plots during the analyzed period, we applied the following conditions to extract the most intense bora and sirocco situations: wind vectors having directions within the 225°–275° azimuth range and speeds exceeding 6 m/s were defined as the bora (401 cases: 7.8% of the time series), while those directed between 315° and 15°, with speeds over 3 m/s were ascribed to the sirocco (524 cases: 10.2% of the series). The comparisons between the bora and the sirocco conditionally averaged surface currents and the averages of the respective BMU time series (weighted by their occurrence) are given in Figure 8.

[40] The resemblance between results obtained by using different methods to extract the most intense bora and sirocco driven surface current patterns is very high. For the bora regime both methods confirm westward and southwestward jet along the northern coast, meridionally decreasing westward flow in the central part and a weak cyclonic recirculation in the southernmost area. The complex correlation between two fields is 0.99, with 2.3° clockwise veering of averaged bora SOM vectors with respect to the bora CAC. The match between the sirocco CAC and averaged sirocco SOMs is also considerable, indicating a more uniform northward flow in the central and southern part, and weaker circulation close to the northern coast. The correlation coefficient is 0.99, while the veering between averaged sirocco SOM vectors and the sirocco CAC is 2.5° in a counterclockwise direction.

4. Summary and Discussion

[41] The study of HF radar measurements presented here focuses on the Adriatic northeasternmost area, which is prone to intense maritime traffic (two very important ports are located in the Gulf of Trieste: Trieste in Italy and Koper in Slovenia) and therefore potentially exposed to a number

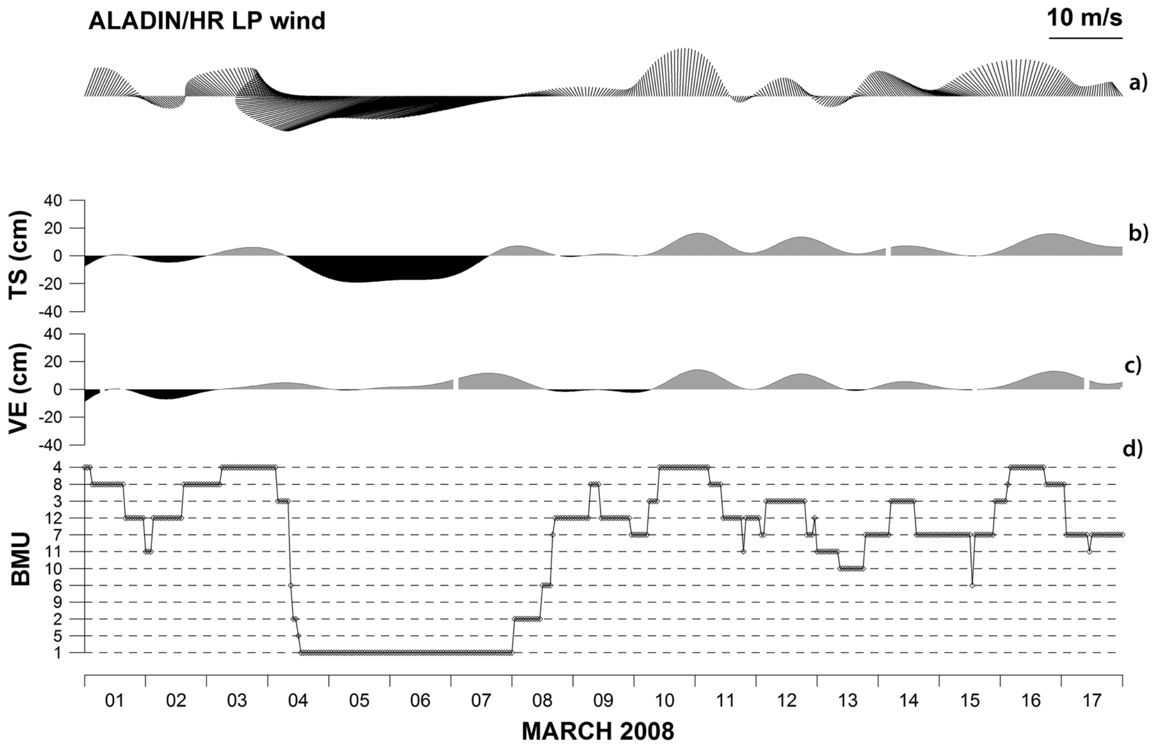

Figure 6. Same as in Figure 5 for the interval between 1 and 17 March 2008.

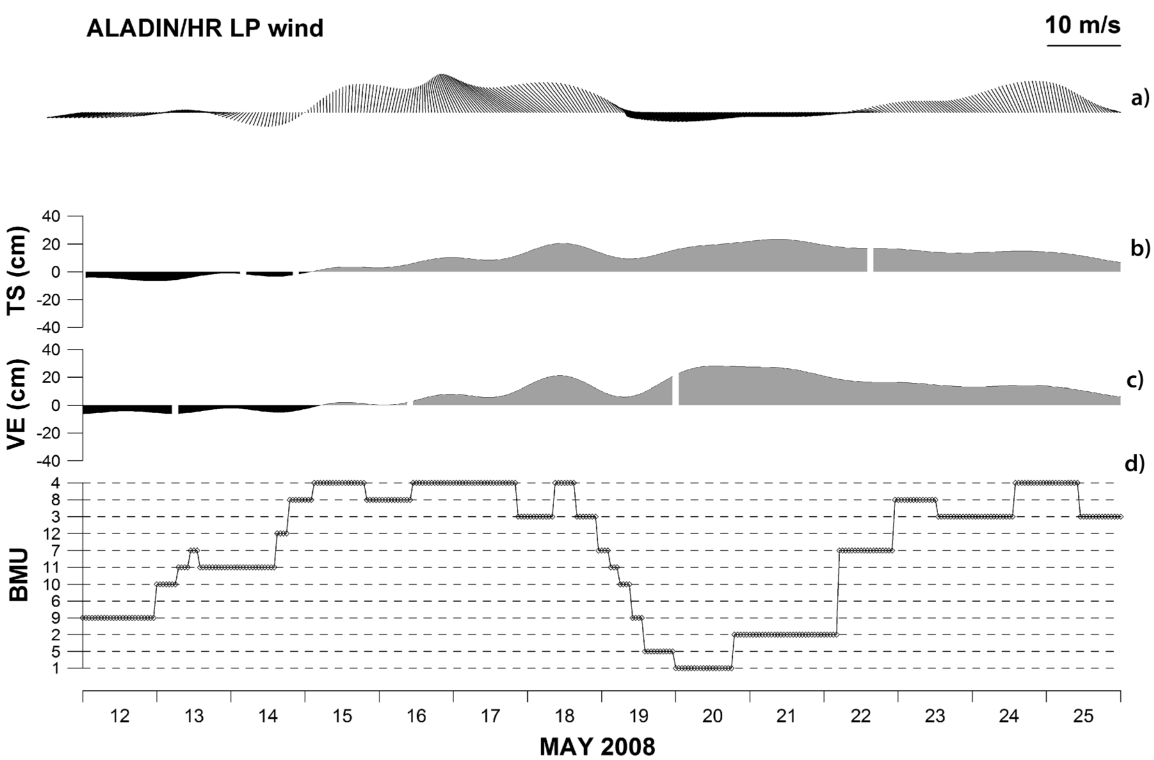

Figure 7. Same as in Figure 5 for the interval extending from 12 to 25 May 2008.

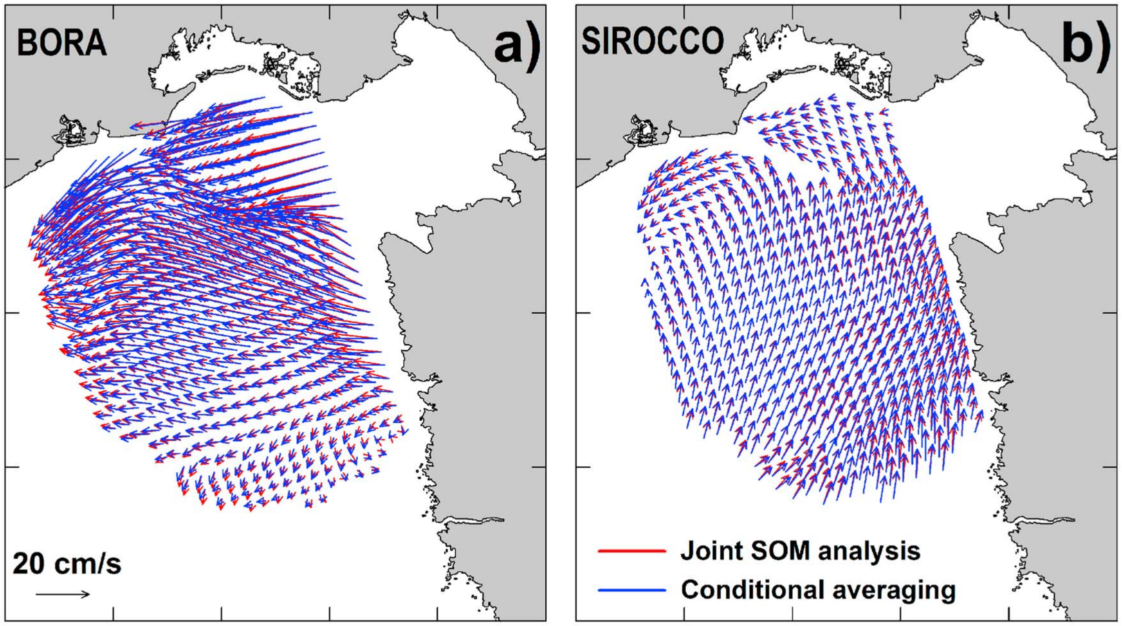

Figure 8. (a) Comparison between conditionally averaged current field for bora wind regime (for low-passed speeds higher than 6 m/s: blue vectors) and the weighted average of corresponding BMU units extracted by joint SOM analysis (red vectors). (b) Same as in Figure 8a, except for sirocco wind conditions (low-passed speeds higher than 3 m/s: blue vectors) and the weighted average of respective SOM units (red vectors).

of pollution sources. An analysis encompassed the February–August 2008 period, when three radars were operational thus providing the best spatial and temporal data coverage. A new method in interpreting HF radar surface currents in the Adriatic was implemented (self-organizing map analysis), offering an insight in characteristic surface current patterns and their temporal evolution.

[42] The SOM proved to be an efficient tool in extracting subtidal surface current features related to the wind dynamics in the area, particularly distinguishing between the two most prominent winds, the bora and the sirocco. Two data arrays were analyzed: one containing only HF radar measurements and the other including HF radar measurements and wind data from the operational mesoscale model ALADIN/HR. The features recognized by the SOMs were very similar, especially for bora and sirocco, having similar spatial characteristics and overall occurrence. Moreover, other winds and calm were described by about 56% of the data. The mapping quality improved when the ALADIN/HR wind data were included in the analysis (lower QE and TE), confirming that the SOM-based approach is quite adequate in obtaining characteristic wind and wind-driven patterns over a limited area of the northern Adriatic.

[43] The strongest bora episode took place at the beginning of March 2008, and the sea surface response was almost instantaneous (mostly described by the SOM unit 1). A strong westward flow along the northern Italian coast was observed, with significant current shear in the southern part and pronounced sea level difference between Trieste and Venice. The response of surface currents to strong sirocco forcing (e.g., mid-May 2008) was more homogenous (BMU4), characterized by relatively uniform northward flow along the western coast of the Istrian Peninsula, while subsiding and changing direction close to the northern shores. The SOM also recognized less pronounced bora and sirocco related patterns, mainly occurring during weaker wind episodes, or reflecting transient states between calmer intervals and the most energetic wind events.

[44] The observed strong correlation between characteristic surface current patterns and dominant winds forecasted by an operational mesoscale meteorological model introduces a possibility for creation of fast and low time-consuming ocean forecast models in the northern Adriatic. Furthermore, we found neural network approach suitable and applicable to such a system, as it introduces low errors in the characteristic patterns and in their evolution in time. Introducing neural networks to the ocean, atmosphere and climate modeling is recently recognized as an effective tool for achievement of rather significant decrease in computing, being a prerequisite for a real-time high-resolution modeling [*Cherkassky et al.*, 2006; *Krasnopolsky*, 2007]. A simple but effective option for the northern Adriatic may be a use of operational meteorological products (e.g., ALADIN/HR) for forecasting characteristic surface current patterns through pattern recognition achieved by the SOM. Precisely, the ALADIN/HR forecasted winds at 10 m at a certain moment may be related to the closest SOM wind pattern, and then to associated surface current pattern. This approach particularly applies to strong wind conditions, which are the most dangerous at sea, increasing risks in coastal activities, marine traffic safety, rescue operations, and other. Especially dangerous can be sudden summertime bora events due to extensive tourism in the area, potentially resulting in human casualties [*Beg Paklar et al.*, 2008]. Such an approach could significantly shorten the decision time during any rescue mission in the area, and hopefully mitigate

potential disasters and accidents on the sea [*Mau et al.*, 2007]. Moreover, long-term HF radar measurements would allow for better (and more detailed) recognition of surface current features, by implementing a larger map size on more complex data sets.

[45] The documented SOM-based forecast may be applicable to any geographical region where correlation between the operational meteorological (or other) forecasted patterns and oceanographic parameters is significant. Also, other related parameters may be assessed and forecasted if they are correlated with the circulation in the area, such as distribution of nutrients and pollutants. For example, phytoplankton blooms and fish catch are impacted by the northern Adriatic circulation [*Kraus and Supić*, 2011], as well as are massive mucilage events [*Grilli et al.*, 2005]. The use of SOM and neural network approaches in the local and basin-wide forecasts is not depending on underlying physics and biogeochemical relations as the method is treating all parameters, relationships and trophic relations as pure numbers; therefore, it could be used operationally for a system of high complexity if possessing enough cross-correlations between the variables. Nevertheless, such an approach should not be used in explaining and understanding of the system functioning, but only for rapid assessment and forecasts studies where SOM is found to significantly decrease the time in which a decision (measure, action) should be agreed upon and implemented.

[46] **Acknowledgments.** We are indebted to Andrea Mazzoldi for his contribution in assuring the continuous radar functioning, system calibration and data collection. Sea level data were provided by the Institute for Environmental Protection and Research, Italy (available at http://www.mareografico.it). Martina Tudor is thanked for providing atmospheric pressure data for February 2008. The SOM Toolbox version 2.0 for Matlab was developed by E. Alhoniemi, J. Himberg, J. Parhankangas, and J. Vesanto at the Helsinki University of Technology, Finland, and is available at http://www.cis.hut.fi/projects/somtoolbox. The comments of two anonymous reviewers helped to improve the original manuscript. This study has been conducted through financial assistance of the European Union (Interreg IIIa Adriatic Cross-Border Programme, project NASCUM, http://www.izor.hr/nascum) and coordinated by Consortium for Coordination of Research Activities Concerning the Venice Lagoon System (CORILA). Additional support was received through the Ministry of Science, Education and Sports of the Republic of Croatia (grants 001-0013077-1122 and 119-1193086-3085).

References

Ainsworth, E. J. (1999), Visualization of ocean colour and temperature from multispectral imagery captured by the Japanese ADEOS satellite, *J. Vis.*, *2*, 195–204, doi:10.1007/BF03181523.

Ainsworth, E. J., and S. F. Jones (1999), Radiance spectra classification from the ocean color and temperature scanner on ADEOS, *IEEE Trans. Geosci. Remote Sens.*, *37*, 1645–1656, doi:10.1109/36.763281.

Artegiani, A., D. Bregant, E. Paschini, N. Pinardi, F. Raicich, and A. Russo (1997), The Adriatic Sea general circulation. Part II: Baroclinic circulation structure, *J. Phys. Oceanogr.*, *27*, 1515–1532, doi:10.1175/1520-0485(1997)027<1515:TASGCP>2.0.CO;2.

Barrick, D. E., and B. J. Lipa (1986), An evaluation of least-squares and closed-form dual-angle methods for CODAR surface-current applications, *IEEE J. Oceanic Eng.*, *11*, 322–326, doi:10.1109/JOE.1986.1145159.

Barrick, D. E., M. W. Evans, and B. L. Weber (1977), Ocean surface currents mapped by radar, *Science*, *198*, 138–144, doi:10.1126/science.198.4313.138.

Beg Paklar, G., V. Isakov, D. Koračin, V. Kourafalou, and M. Orlić (2001), A case study of bora-driven flow and density changes on the Adriatic shelf (January 1987), *Cont. Shelf Res.*, *21*, 1751–1783, doi:10.1016/S0278-4343(01)00029-2.

Beg Paklar, G., N. Žagar, M. Žagar, R. Vellore, D. Koračin, P.-M. Poulain, M. Orlić, I. Vilibić, and V. Dadić (2008), Modeling the trajectories of satellite-tracked drifters in the Adriatic Sea during a summertime bora event, *J. Geophys. Res.*, *113*, C11S04, doi:10.1029/2007JC004536.

Book, J. W., H. T. Perkins, L. Cavaleri, J. D. Doyle, and J. D. Pullen (2005), ADCP observations of the western Adriatic slope current during winter of 2001, *Prog. Oceanogr.*, *66*, 270–286, doi:10.1016/j.pocean.2004.07.014.

Buljan, M., and M. Zore-Armanda (1976), Oceanographic properties of the Adriatic Sea, *Oceanogr. Mar. Biol.*, *14*, 11–98.

Cavazos, T. (2000), Using self-organizing maps to investigate extreme climate events: An application to wintertime precipitation in the Balkans, *J. Clim.*, *13*, 1718–1732, doi:10.1175/1520-0442(2000)013<1718:USOMTI>2.0.CO;2.

Chapman, R. D., and H. C. Graber (1997), Validation of HF radar measurements, *Oceanography*, *10*(2), 76–79.

Chavanne, C., I. Janeković, P. Flament, P.-M. Poulain, M. Kuzmić, and K.-W. Gurgel (2007), Tidal currents in the northwestern Adriatic: High-frequency radio observations and numerical model predictions, *J. Geophys. Res.*, *112*, C03S21, doi:10.1029/2006JC003523.

Cherkassky, V., V. M. Krasnopolsky, D. P. Solomatine, and J. Valdes (2006), Computational intelligence in earth sciences and environmental applications: Issues and challenges, *Neural Netw.*, *19*, 113–121, doi:10.1016/j.neunet.2006.01.001.

Cosoli, S., M. Gačić, and A. Mazzoldi (2005), Comparison between HF radar current data and moored ADCP currentmeter, *Nuovo Cimento*, *28C*(6), 865–879, doi:10.1393/noc/i200510032-6.

Cosoli, S., A. Mazzoldi, and M. Gačić (2010), Validation of surface current measurements in the northern Adriatic Sea from high-frequency radars, *J. Atmos. Oceanic Technol.*, *27*, 908–919, doi:10.1175/2009JTECHO680.1.

Courtier, P., C. Freydier, J.-F. Geleyn, F. Rabier, and M. Rochas (1991), The ARPEGE project at METEO-FRANCE, in *Proceedings of the ECMWF Seminar on Numerical Methods in Atmospheric Models*, vol. 2, pp. 192–231, ECMWF, Reading, U. K.

Crombie, D. D. (1955), Doppler spectrum of sea echo at 13.56 Mc/s, *Nature*, *175*, 681–682, doi:10.1038/175681a0.

Cushman-Roisin, B., and K. A. Korotenko (2007), Mesoscale-resolving simulations of summer and winter bora events in the Adriatic Sea, *J. Geophys. Res.*, *112*, C11S91, doi:10.1029/2006JC003516.

Emery, W. J., and R. E. Thomson (1997), Data Analysis Methods in Physical Oceanography, 634 pp., Pergamon, Oxford, U. K.

Gačić, M., P.-M. Poulain, M. Zore-Armanda, and V. Barale (2001), Overview, in *Physical Oceanography of the Adriatic Sea*, edited by B. Cushman-Roisin et al., pp. 1–44, Kluwer Acad., Dordrecht, Netherlands.

Gačić, M., V. Kovačević, S. Cosoli, A. Mazzoldi, J. D. Paduan, I. Mancero Mosquera, and S. Yari (2009), Surface current patterns in front of the Venice Lagoon, *Estuarine Coastal Shelf Sci.*, *82*, 485–494, doi:10.1016/j.ecss.2009.02.012.

Grilli, F., E. Paschini, R. Precali, A. Russo, and N. Supić (2005), Circulation and horizontal fluxes in the northern Adriatic Sea in the period June 1999–July 2002. Part I: Geostrophic circulation and current measurement, *Sci. Total Environ.*, *353*, 57–67, doi:10.1016/j.scitotenv.2005.09.008.

Grisogono, B., and D. Belušić (2009), A review of recent advances in understanding the meso and microscale properties of the severe Bora wind, *Tellus, Ser. A*, *61*, 1–16.

Gurgel, K.-W., H.-H. Essen, and S. P. Kingsley (1999), HF radars: Physical limitations and recent developments, *Coastal Eng.*, *37*, 201–218, doi:10.1016/S0378-3839(99)00026-5.

Gurgel, K.-W., H.-H. Essen, and T. Schlick (2006), An empirical method to derive ocean waves from second-order Bragg scattering: Prospects and limitations, *IEEE J. Oceanic Eng.*, *31*, 804–811, doi:10.1109/JOE.2006.886225.

Hewitson, B. C., and R. G. Crane (2002), Self-organizing maps: Applications to synoptic climatology, *Clim. Res.*, *22*, 13–26, doi:10.3354/cr022013.

Hydrographic Institute of the Republic of Croatia (2010), *Report on Tide-Gauge Measurements on the East Adriatic Coast for 2008*, 50 pp., Split, Croatia.

Ivatek-Šahdan, S., and M. Tudor (2004), Use of high-resolution dynamical adaptation in operational suite and research impact studies, *Meteorol. Z.*, *13*(2), 99–108, doi:10.1127/0941-2948/2004/0013-0099.

Kohonen, T. (1982), Self-organized information of topologically correct features maps, *Biol. Cybern.*, *43*, 59–69, doi:10.1007/BF00337288.

Kohonen, T. (2001), *Self-Organizing Maps*, *Springer Ser. Inf. Sci.*, vol. 30, 3rd ed., 501 pp., Springer, New York.

Kovačević, V., M. Gačić, A. Mazzoldi, G. Dallaporta, and A. Gaspari (2000), Sea-surface currents measured by coastal HF radar offshore Ancona, *B. Geofis. Teor. Appl.*, *41*, 339–355.

Kovačević, V., M. Gačić, I. Mancero Mosquera, A. Mazzoldi, and S. Marinetti (2004), HF radar observations in the northern Adriatic: Surface current field in front of the Venetian Lagoon, *J. Mar. Syst.*, *51*, 95–122, doi:10.1016/j.jmarsys.2004.05.026.

Krasnopolsky, V. M. (2007), Neural network emulations for complex multidimensional geophysical mappings: Applications of neural network techniques to atmospheric and oceanic satellite retrievals and numerical modelling, *Rev. Geophys.*, *45*, RG3009, doi:10.1029/2006RG000200.

Kraus, R., and N. Supić (2011), Impact of circulation on high phytoplankton blooms and fish catch in the northern Adriatic (1990–2004), *Estuarine Coastal Shelf Sci.*, *91*, doi:10.1016/j.ecss.2010.10.021.

Kundu, P. K. (1976), Ekman veering observed near the ocean bottom, *J. Phys. Oceanogr.*, *6*, 238–242, doi:10.1175/1520-0485(1976)006<0238:EVONTO>2.0.CO;2.

Lipa, B. J., and D. E. Barrick (1983), Least-squares methods for the extraction of surface currents from CODAR crossed-loop data: Application at ARSLOE, *IEEE J. Oceanic Eng.*, *8*, 226–253, doi:10.1109/JOE.1983.1145578.

Lipa, B. J., D. E. Barrick, J. Bourg, and B. B. Nyden (2006), HF radar detection of tsunamis, *J. Oceanogr.*, *62*(5), 705–716, doi:10.1007/s10872-006-0088-9.

Liu, Y., and R. H. Weisberg (2005), Patterns of ocean current variability on the West Florida Shelf using the self-organizing map, *J. Geophys. Res.*, *110*, C06003, doi:10.1029/2004JC002786.

Liu, Y., and R. H. Weisberg (2007), Ocean currents and sea surface heights estimated across the West Florida Shelf, *J. Phys. Oceanogr.*, *37*, 1697–1713, doi:10.1175/JPO3083.1.

Liu, Y., and R. H. Weisberg (2011), A review of self-organizing map applications in meteorology and oceanography, in *Self-Organizing Maps: Applications and Novel Algorithm Design*, edited by J. I. Mwasiagi, pp. 253–272, InTech, Rijeka, Croatia.

Liu, Y., R. H. Weisberg, and R. He (2006a), Sea surface temperature patterns on the West Florida Shelf using the growing hierarchical self-organizing maps, *J. Atmos. Oceanic Technol.*, *23*, 325–338, doi:10.1175/JTECH1848.1.

Liu, Y., R. H. Weisberg, and C. N. K. Mooers (2006b), Performance evaluation of the self-organizing map for feature extraction, *J. Geophys. Res.*, *111*, C05018, doi:10.1029/2005JC003117.

Liu, Y., R. H. Weisberg, and L. K. Shay (2007), Current patterns on the West Florida Shelf from joint self-organizing map analyses of HF radar and ADCP data, *J. Atmos. Oceanic Technol.*, *24*, 702–712, doi:10.1175/JTECH1999.1.

Malanotte-Rizzoli, P., and A. Bergamasco (1983), The dynamics of the coastal region of the northern Adriatic Sea, *J. Phys. Oceanogr.*, *13*, 1105–1130, doi:10.1175/1520-0485(1983)013<1105:TDOTCR>2.0.CO;2.

Malmgren, B. A., and A. Winter (1999), Climate zonation in Puerto Rico based on principal components analysis and an artificial neural network, *J. Clim.*, *12*, 977–985, doi:10.1175/1520-0442(1999)012<0977:CZIPRB>2.0.CO;2.

Mau, J.-C., D.-P. Wang, D. S. Ullman, and D. L. Codiga (2007), Characterizing Long Island Sound outflows from HF radar using self-organizing maps, *Estuarine Coastal Shelf Sci.*, *74*, 155–165, doi:10.1016/j.ecss.2007.04.007.

Meteorological and Hydrological Service of Croatia (2008), Bulletin on meteorology, hydrology, applied meteorology and environmental protection: February (in Croatian), 48 pp., Zagreb.

Orlić, M., M. Gačić, and P. E. La Violette (1992), The currents and circulation of the Adriatic Sea, *Oceanol. Acta*, *15*(2), 109–124.

Orlić, M., M. Kuzmić, and Z. Pasarić (1994), Response of the Adriatic Sea to the bora and sirocco forcing, *Cont. Shelf Res.*, *14*, 91–116, doi:10.1016/0278-4343(94)90007-8.

Paduan, J. D., and H. C. Graber (1997), Introduction to high frequency radar: Reality and myth, *Oceanography*, *10*(2), 36–39.

Paduan, J. D., and L. K. Rosenfeld (1996), Remotely sensed surface currents in Monterey Bay from shore-based HF radar (CODAR), *J. Geophys. Res.*, *101*, 20,669–20,686, doi:10.1029/96JC01663.

Pasarić, Z., D. Belušić, and Z. B. Klaić (2007), Orographic influences on the Adriatic sirocco wind, *Ann. Geophys.*, *25*, 1263–1267, doi:10.5194/angeo-25-1263-2007.

Pawlowicz, R., B. Beardsley, and S. Lentz (2002), Classical tidal harmonic analysis including error estimates in MATLAB using T_TIDE, *Comput. Geosci.*, *28*, 929–937, doi:10.1016/S0098-3004(02)00013-4.

Poulain, P.-M. (2001), Adriatic Sea surface circulation as derived from drifter data between 1990 and 1999, *J. Mar. Syst.*, *29*, 3–32, doi:10.1016/S0924-7963(01)00007-0.

Poulain, P.-M., and B. Cushman-Roisin (2001), Circulation, in *Physical Oceanography of the Adriatic Sea*, edited by B. Cushman-Roisin et al., pp. 67–110, Kluwer Acad., Dordrecht, Netherlands.

Poulain, P.-M., and F. Raicich (2001), Forcings, in *Physical Oceanography of the Adriatic Sea*, edited by B. Cushman-Roisin et al., pp. 45–65, Kluwer Acad., Dordrecht, Netherlands.

Poulain, P.-M., V. K. Kourafalou, and B. Cushman-Roisin (2001), Nothern Adriatic Sea, in *Physical Oceanography of the Adriatic Sea*, edited by B. Cushman-Roisin et al., pp. 143–165, Kluwer Acad., Dordrecht, Netherlands.

Poulain, P.-M., E. Mauri, and L. Ursella (2004), Unusual upwelling event and current reversal off the Italian Adriatic coast in summer 2003, *Geophys. Res. Lett.*, *31*, L05303, doi:10.1029/2003GL019121.

Reusch, D. B., R. B. Alley, and B. C. Hewitson (2007), North Atlantic climate variability from a self-organizing map perspective, *J. Geophys. Res.*, *112*, D02104, doi:10.1029/2006JD007460.

Richardson, A. J., M. C. Pfaff, J. G. Field, N. F. Silulwane, and F. A. Shillington (2002), Identifying characteristic chlorophyll *a* profiles in the coastal domain using an artificial neural network, *J. Plankton Res.*, *24*, 1289–1303, doi:10.1093/plankt/24.12.1289.

Richardson, A. J., C. Risien, and F. A. Shillington (2003), Using self-organizing maps to identify patterns in satellite imagery, *Prog. Oceanogr.*, *59*, 223–239, doi:10.1016/j.pocean.2003.07.006.

Risien, C. M., C. J. C. Reason, F. A. Shillington, and D. B. Chelton (2004), Variability in satellite winds over the Benguela upwelling system during 1999–2000, *J. Geophys. Res.*, *109*, C03010, doi:10.1029/2003JC001880.

Silulwane, N. F., A. J. Richardson, F. A. Shillington, and B. A. Mitchell-Innes (2001), Identification and classification of vertical chlorophyll patterns in the Benguela upwelling system and Angola-Benguela Front using an artificial neural network, *S. Afr. J. Mar. Sci.*, *23*, 37–51.

Socal, G., et al. (2008), Hydrological and biogeochemical features of the northern Adriatic Sea in the period 2003–2006, *Mar. Ecol. Evol. Perspective.*, *29*, 449–468.

Solidoro, C., V. Bandelj, P. Barbieri, G. Cossarini, and S. F. Umani (2007), Understanding dynamic of biogeochemical properties in the northern Adriatic Sea by using self-organizing maps and k-means clustering, *J. Geophys. Res.*, *112*, C07S90, doi:10.1029/2006JC003553.

Ursella, L., P.-M. Poulain, and R. P. Signell (2006), Surface drifter derived circulation in the northern and middle Adriatic Sea: Response to wind regime and season, *J. Geophys. Res.*, *111*, C03S04, doi:10.1029/2005JC003177 [printed *112*(C3), 2007].

Vesanto, J., and E. Alhoniemi (2000), Clustering of the self-organizing map, *IEEE Trans. Neural Netw.*, *11*(3), 586–600, doi:10.1109/72.846731.

Vesanto, J., J. Himberg, E. Alhoniemi, and J. Parhankangas (2000), SOM Toolbox for Matlab 5, *Tech. Rep. A57*, *FIN-02015 HUT*, 59 pp., Helsinki Univ. of Technol., Helsinki.

Vilibić, I. (2006), The role of the fundamental seiche in the Adriatic coastal floods, *Cont. Shelf Res.*, *26*, 206–216, doi:10.1016/j.csr.2005.11.001.

Vilibić, I., V. Dadić, D. Ivanković, S. Muslim, J. Šepić, and H. Mihanović (2009), Real-time procedures implemented within coastal HF radar system in the northern Adriatic, in *Oceans 2009– Europe*, vols. 1 and 2, pp. 1121–1126, IEEE, New York, doi:10.1109/OCEANSE.2009.5278351.

Vilibić, I., H. Mihanović, J. Šepić, and S. Matijević (2011), Using self-organising maps to investigate long-term changes in deep Adriatic water patterns, *Cont. Shelf Res.*, *31*, 695–711, doi:10.1016/j.csr.2011.01.007.

Wyatt, L. R. (2005), HF radar for coastal monitoring: A comparison of methods and measurements, in *Oceans 2005–Europe*, vol. 1, edited by IEEE, pp. 314–318, IEEE, New York, doi:10.1109/OCEANSE.2005.1511732.

S. Cosoli and M. Gačić, OGS, Borgo Grotta Gigante 42/C, I-34010 Sgonico, Trieste, Italy.

V. Dadić, D. Ivanković, and I. Vilibić, Institute of Oceanography and Fisheries, Šetalište I. Meštrovića 63, 21000 Split, Croatia.

H. Mihanović, Hydrographic Institute of the Republic of Croatia, Zrinsko-Frankopanska 161, 21000 Split, Croatia. (hrvoje.mihanovic@hhi.hr)